Walisongo Journal of Chemistry
Walisongo Journal of Chemistry Vol. 9 Issue 1 (2026), 54-66
ISSN: 2621-5985 (online); 2549-385X (print)
DOI: https://doi.org/10.21580/wjc.v9i1.31583

ADSORPTION BEHAVIOR OF Pb (II) ON GAMALAMA VOLCANIC SOIL: KINETIC AND ISOTHERM STUDIES

Indra Cipta[1]*, Nur Jannah Baturante[1], Hernawan[2], M. Hidayat Jaya Miharja[1], Nur Fadillah Putri Saiful[3]

[1]Department of Chemistry Education, Faculty of Teacher Training and Education, Universitas Khairun, Indonesia
[2]Research Center for Food Technology and Processing, National Research and Innovation Agency, Indonesia
[3]Undergraduate Program Student, Department of Chemistry Education, Faculty of Teacher Training and Education, Universitas Khairun, Indonesia

*Corresponding author: indra.chemy@gmail.com

Abstract

Lead (Pb) contamination in aquatic environments poses serious risks to ecosystems and human health due to its toxicity and persistence. This study evaluates the potential of Gamalama volcanic soil (GVS), a locally abundant aluminosilicate material, as a low-cost adsorbent for Pb(II) removal. Batch adsorption experiments were conducted at initial Pb(II) concentrations of 50–500 mg/L and contact times of 20–120 min. Adsorption behavior was analyzed using kinetic models, namely the pseudo-first-order and pseudo-second-order models, and isotherm models, namely the Langmuir and Freundlich models. The structural and surface properties of GVS before and after adsorption were characterized by FTIR, XRD, and N_2 adsorption (BET). The adsorption efficiency decreased from 45.8% to 33.6% with increasing initial Pb(II) concentration, indicating progressive saturation of active sites. In contrast, adsorption increased with contact time and reached a maximum of 94.87% at 60 min. Kinetic analysis showed an excellent fit to the pseudo-second-order model (R^2 = 0.9997), suggesting a chemisorption-controlled process. The Freundlich isotherm provided a better fit (R^2 = 0.9902), indicating multilayer adsorption on heterogeneous surfaces. XRD patterns showed no significant changes after adsorption, while the BET surface area decreased from 490.128 to 464.707 m^2/g, suggesting partial pore blockage. These results demonstrate that GVS is a promising natural adsorbent for Pb(II) removal, although further studies on selectivity and regeneration are required for practical applications.

Keywords: *Adsorption, Gamalama volcanic soil, Pseudo-second-order model, Freundlich isotherm, Low-cost adsorbent*

Introduction

The increase in mining activity in Indonesia in recent years has been accompanied by increasing heavy metal pollution in the environment. The discharge of heavy metals can harm ecosystems and human health [1], [2]. One of the most dangerous heavy metals is lead (Pb), which is persistent, very difficult to degrade naturally, and tends to accumulate in soil, sediment, and aquatic systems. The presence of Pb at certain concentrations can inhibit plant growth, disrupt soil nutrient balance, and endanger ecosystems. The bioaccumulation of lead in the food chain ultimately increases human exposure, posing serious health risks such as neurological impairment, cardiovascular

problems, kidney damage, and immune dysfunction. Children exposed to lead are particularly vulnerable to developmental and cognitive deficits [3], [4], [5]. These impacts highlight the urgent need for effective and sustainable Pb remediation strategies.

Heavy metal removal technologies are well known and widely applied, particularly chemical precipitation [6], ion exchange [7], [8], membrane separation [10], [11], and adsorption techniques [12], [13]. Among these removal techniques, adsorption has been extensively investigated and is considered a favorable method because of its simplicity, low operational cost, and high efficiency [14], [15], [16]. Previous studies have highlighted the capacity of clay minerals, such as allophane, halloysite, and kaolinite, to bind heavy metal ions through their high surface area and reactive functional groups. However, most studies have focused on chemically modified or purified adsorbents, while only a limited number have examined the adsorption potential of naturally occurring, unmodified volcanic soils.

In Indonesia, the Ternate region in North Maluku is particularly vulnerable to heavy metal contamination due to intensive mining activities. Therefore, a removal material that is both effective and locally accessible is urgently needed. Gamalama volcanic soil (GVS) is abundant in this region and contains aluminosilicate minerals such as allophane, halloysite, and silica, which are known to possess high surface areas and reactive surface hydroxyl groups suitable for heavy metal adsorption [17], [18], [19], [20]. Previous studies have reported the adsorption potential of purified clay, aluminosilicate minerals, and chemically modified adsorbents for Pb(II) removal [5], [21], [22]. However, studies on the direct utilization of natural, unmodified volcanic soil as a Pb(II) adsorbent remain limited. Moreover, evidence regarding the adsorption mechanism, kinetic behavior, and mineral and structural stability of Gamalama volcanic soil after Pb adsorption is still insufficient. Thus, this study aims to evaluate the adsorption performance of natural Gamalama volcanic soil for Pb(II) removal. Specifically, this study focuses on: (1) investigating adsorption behavior under varying initial Pb concentrations and contact times; (2) analyzing the adsorption mechanism using the Langmuir and Freundlich isotherm models; (3) determining adsorption kinetics using the pseudo-first-order and pseudo-second-order models; and (4) assessing the structural and mineralogical changes of the adsorbent using FTIR, XRD, and SAA–BET characterization.

Methodology

The materials used in this study included GVS, hydrogen peroxide, $Pb(NO_3)_2$, NaCl, HCl, NaOH, and distilled water. All chemicals used were of analytical grade and obtained from Merck. GVS was collected from 0°50’12.3" N, 127°19’18.6" E, Ternate, North Maluku, at a depth of 0–70 cm. The soil was then air-dried and ground to a particle size of 200 mesh. To remove organic content, 20 g of soil was stirred with 200 mL of distilled water and reacted with 10 mL of 30% hydrogen peroxide. The solid was then dried at 80°C for 3 h.

The point of zero charge pH (pH_{pzc}) of GVS was determined using the pH drift method in 25 mL of 0.1 M NaCl solution. A series of NaCl solutions with different initial pH values was prepared using HCl and NaOH, followed by the addition of 20 mg of GVS. After 12 h, the final pH was measured, and pH_{pzc} was determined from the point at which $\Delta pH = 0$.

A total of 20 mg of GVS was added to 25 mL of Pb(II) solution at pH 6 with varying concentrations of 50, 100, 200, 300, and 500 ppm. The contact times used in this study were 20, 30, 40, 60, and 120 min to study the adsorption kinetics. The adsorption experiments were conducted by adding 20 mg of the GVS adsorbent to 25 mL of Pb(II) solution. To determine the effect of Pb adsorption on the structure and minerals of GVS, FTIR, XRD, and SAA–BET characterization of GVS was carried out before and after adsorption.

FTIR analysis was performed using a Shimadzu FTIR spectrophotometer (model 8201PC) over a wavenumber range of 300–

4000 cm^{-1}. The spectra of all samples were obtained using the KBr pellet method. X-ray diffraction (XRD) patterns were recorded using a Shimadzu diffractometer (model 6000) with Cu Kα radiation. The data were collected over a 2θ range of 3–80° in continuous scan mode, with a scanning rate of 3° min^{-1}, a sampling pitch of 0.02°, and a preset time of 0.40 s. The specific surface area of the samples was determined by N_2 adsorption at 77.3 K using the BET method with a Quantachrome Instruments Nova analyzer. The pressure tolerance was set at 0.100/0.100 for adsorption/desorption measurements.

The adsorption data were analyzed using pseudo-first-order (PFO) [23] and pseudo-second-order (PSO) [24] kinetic models to evaluate the adsorption rate and possible controlling mechanisms. The PFO equation is expressed as follows:

$$\text{Ln}\,(q_e - q_t) = \ln q_e - k_1 t \quad \text{.....(1)}$$

The PSO equation is expressed as follows:

$$\frac{t}{q_t} = \frac{1}{k_2 q_e^2} + \frac{t}{q_e} \quad \text{... ... ... (2)}$$

where q_t (mg g^{-1}) is the adsorption capacity at time t, q_e (mg g^{-1}) is the adsorption capacity at equilibrium, k_1 (min^{-1}) is the rate constant of the pseudo-first-order model, and k_2 (g mg^{-1} min^{-1}) is the rate constant of the pseudo-second-order model. Equilibrium adsorption data were analyzed using the Langmuir and Freundlich isotherm models. The Langmuir model equation is expressed as follows:

$$\frac{C_e}{q_e} = \frac{1}{q_{max} k_l} + \frac{C_e}{q_{max}} \quad \text{... ... ... (3)}$$

The Freundlich linear equation is expressed as follows:

$$\log q_e = \log K_F + \frac{1}{n} log C_e \quad \text{... ... ... (4)}$$

where C_e is the Pb(II) concentration at equilibrium (mg L^{-1}), Qmax is the theoretical monolayer adsorption capacity estimated by the Langmuir model (mg g^{-1}), KL is the Langmuir constant, and KF is the Freundlich constant.

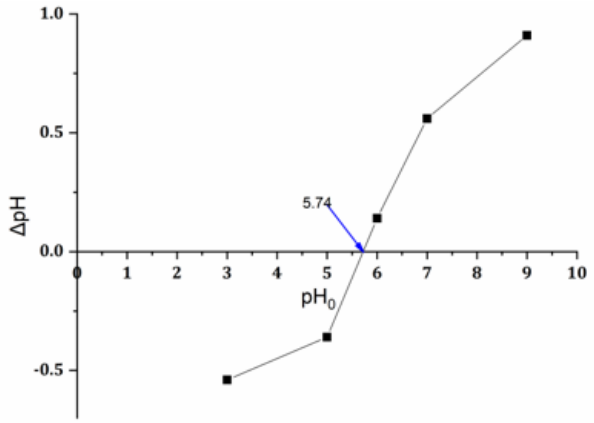

Figure 1. Gamalama volcanic soil pH_{pzc}

Results and Discussion

In this study, the kinetics of Pb adsorption using Gamalama volcanic soil were studied using pseudo-first-order and pseudo-second-order equations. Furthermore, the adsorption data were also analyzed using the Langmuir [25] and Freundlich isotherms [26] to study the adsorption mechanism. The pH_pzc of GVS was estimated to be approximately 5.74 (Fig. 1). The pH_pzc value indicates that the adsorbent surface becomes increasingly negative above this pH, which is more suitable for the adsorption of Pb^{2+} ions through electrostatic attraction. Therefore, in this study, pH 6 favored Pb(II) adsorption while minimizing hydroxide precipitation.

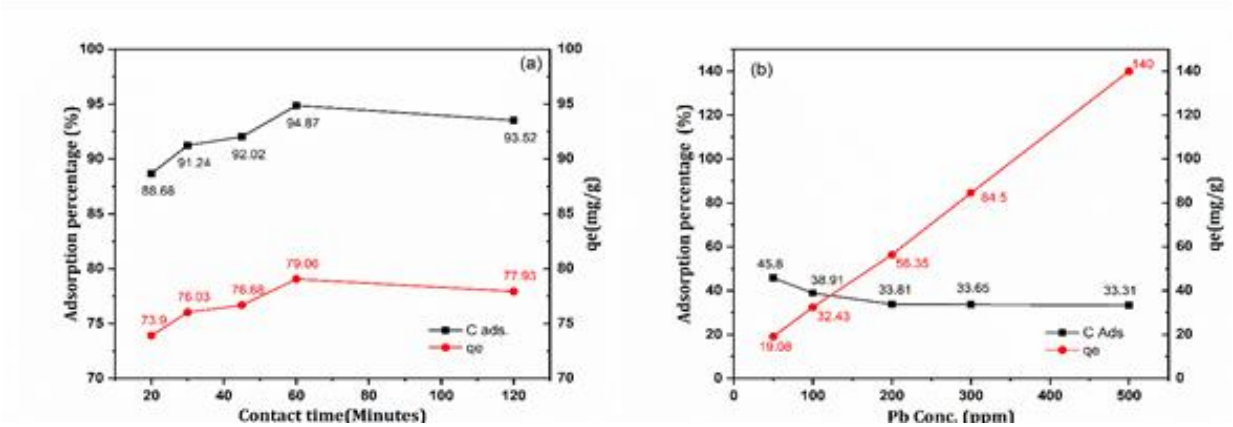

Figure 2. Pb(II) adsorption onto Gamalama volcanic soil: (a) effect of contact time; (b) effect of initial concentration

Pb(II) Adsorption

The adsorption process occurred very rapidly during the first 20–30 min (see Figure 2a). The highest adsorption percentage was achieved at a contact time of 60 min. At 20 min, the adsorption process removed 88.68% of Pb, which further increased to 91.24% at 30 min. This indicates that the adsorbent surface possessed a large number of active sites that were immediately occupied by Pb(II) ions. Adsorption at the initial stage was dominated by rapid diffusion and the interaction of Pb(II) ions with active functional groups, particularly Al–O/Al–OH and Si–O/Si–OH groups. These active sites are abundantly available on the surface of Gamalama volcanic soil. Extending the adsorption contact time to 45 min resulted in a slight increase in adsorption percentage to 92.02%, and at 60 min, adsorption reached its maximum value of 94.87%. This suggests that adsorption equilibrium was reached at a contact time of approximately 60 min. The effect of the initial Pb concentration on adsorption percentage is shown in Figure 2a. Based on Figure 2a, increasing the initial Pb concentration decreased the adsorption percentage. The adsorption percentages were 45.8%, 38.91%, 33.82%, 33.8%, and 33.6% for initial Pb concentrations of 50, 100, 200, 300, and 500 ppm, respectively.

The increase in the initial concentration of Pb was inversely proportional to the Pb adsorption percentage using GVS. As the initial Pb concentration increased from 50 to 500 ppm, the adsorption percentage decreased from 45.8% to 33.6%, suggesting that the adsorbent performs more efficiently at lower concentration levels. This trend is commonly associated with the saturation of functional groups and the limited availability of active adsorption sites on the Gamalama volcanic soil surface [27], [28].

Further contact time to 120 minutes gave Further extension of the contact time to 120 min caused the adsorption percentage to decrease to 93.52%. This slight decrease in adsorption efficiency at 120 min, from 94.87% to 93.52%, may be attributed to desorption and re-equilibration processes, in which weakly bound Pb(II) ions are released back into the solution. In addition, prolonged contact time may lead to the redistribution of Pb(II) ions within the adsorbent pores, resulting in a dynamic equilibrium between adsorption and desorption processes. Similar results have been reported by [29], [30], and [31]. The adsorption capacity increased rapidly during the initial stage and reached a maximum value of 118.59 mg/g at 60 min, indicating rapid occupation of available active sites. A slight decrease at 120 min may be associated with desorption due to re-equilibration processes.

At lower concentrations, the number of Pb(II) ions in the solution was still proportional to the availability of active sites, resulting in relatively high adsorption efficiency. However, as the concentration increased, these sites gradually became occupied, causing intense competition among

Pb ions to bind to the adsorbent surface. The declining trend in adsorption percentage at higher concentrations also suggests that the adsorption process may shift from a high-affinity interaction to a diffusion-limited phase, especially once equilibrium is approached [32], [33]. Although the percentage removal decreased with increasing initial Pb(II) concentration, the adsorption capacity (q_e) increased markedly from 28.63 to 140 mg/g as the concentration increased from 50 to 500 mg/L. This trend indicates that higher Pb(II) concentrations provide a stronger concentration gradient and increase the amount of Pb(II) adsorbed per unit mass of GVS.

To evaluate the practical performance of GVS, the adsorption capacity obtained in this study was compared with those of previously reported natural adsorbents for Pb(II) removal. The experimental adsorption capacity of GVS reached 140 mg/g, which is comparable to those of other silica- or aluminosilicate-based adsorbents, such as bentonite, zeolite, mesoporous silica, clinoptilolite, and metakaolin. The relatively strong performance of GVS may be attributed to its large BET surface area (490 m^2/g) and the presence of reactive mineral phases such as allophane and halloysite. The BET surface area of GVS is relatively higher than those of most of the aforementioned adsorbents. A comparison of the adsorption performance of GVS with those of other natural adsorbents reported in the literature is shown in Table 1. Based on the adsorption capacity and BET surface area shown in Table 1, GVS has strong potential as a local North Maluku adsorbent for Pb(II) removal from aqueous systems.

Adsorption Kinetic Model

Figure 3a and 3b show that the R^2 value for the PSO model was 0.9997, while the R^2 value for the PFO model was only 0.4605. Based on this result, it can be concluded that the Pb(II) adsorption kinetics using GVS are more consistent with the PSO model than with the PFO model. This indicates that the Pb adsorption process by GVS occurs through chemisorption involving the interaction of Pb with active sites on GVS, such as Al–O and Si–O groups.

This finding was further supported by BET analysis, which demonstrated a moderate decrease in surface area from 490.128 to 464.707 m^2/g after adsorption. This reduction in surface area suggests that partial pore blocking and active site occupation occurred during adsorption. In contrast, the pseudo-first-order model showed a poor correlation (R^2 = 0.4605), confirming that the process was not merely diffusion-controlled. Regarding the equilibrium behavior, the adsorption data exhibited a weak correlation with the Langmuir model (R^2 = 0.6179), while the Freundlich model provided an excellent fit (R^2 = 0.9902), with a KF value of 1.989 (Figures 3c and 3d). The Langmuir model showed a relatively poor fit (R^2 = 0.6179), indicating that its assumption of monolayer adsorption on a homogeneous surface is not suitable for this adsorption system. In contrast, the better agreement with the Freundlich model (R^2 = 0.9902) suggests that the GVS surface is heterogeneous and contains different types of active sites, which is reasonable given the presence of multiple mineral phases, such as allophane and halloysite. This behavior is commonly observed in natural adsorbents such as volcanic soils [24], [25], [27], [35], [36].

The utilization of Gamalama volcanic soil showed high potential as a cost-effective and environmentally benign adsorbent for Pb(II) remediation. The rapid adsorption kinetics over a short contact time make the adsorbent highly suitable for short-residence-time treatment systems. For industrial wastewater treatment, this characteristic is ideal for continuous-flow reactors or fixed-bed column systems. The high adsorption efficiency at low Pb concentrations is suitable for the polishing stage of treatment processes, where heavy metal concentrations have already been reduced but must still meet regulatory discharge limits. Meanwhile, the gradual decrease in percentage removal at higher concentrations suggests that multistage adsorption, dose optimization, or adsorbent regeneration strategies may be required when treating wastewater with high Pb loads.

Table 1. Comparison of Pb(II) adsorption capacity and BET surface area of GVS with other adsorbents

Adsorbent	BET Surface Area (m^2/g)	Adsorption capacity (mg/g)	Reference
GVS	490	140	This study
South African bentonitic clay	37.05	4.2	[21]
Zeolite	28.12	66.96	[34]
Mesoporous silica MCM-48	511	127.24	[35]
Clinoptilolite	21	32	[36]
Metakaolin geopolymer	64.7	100	[37]

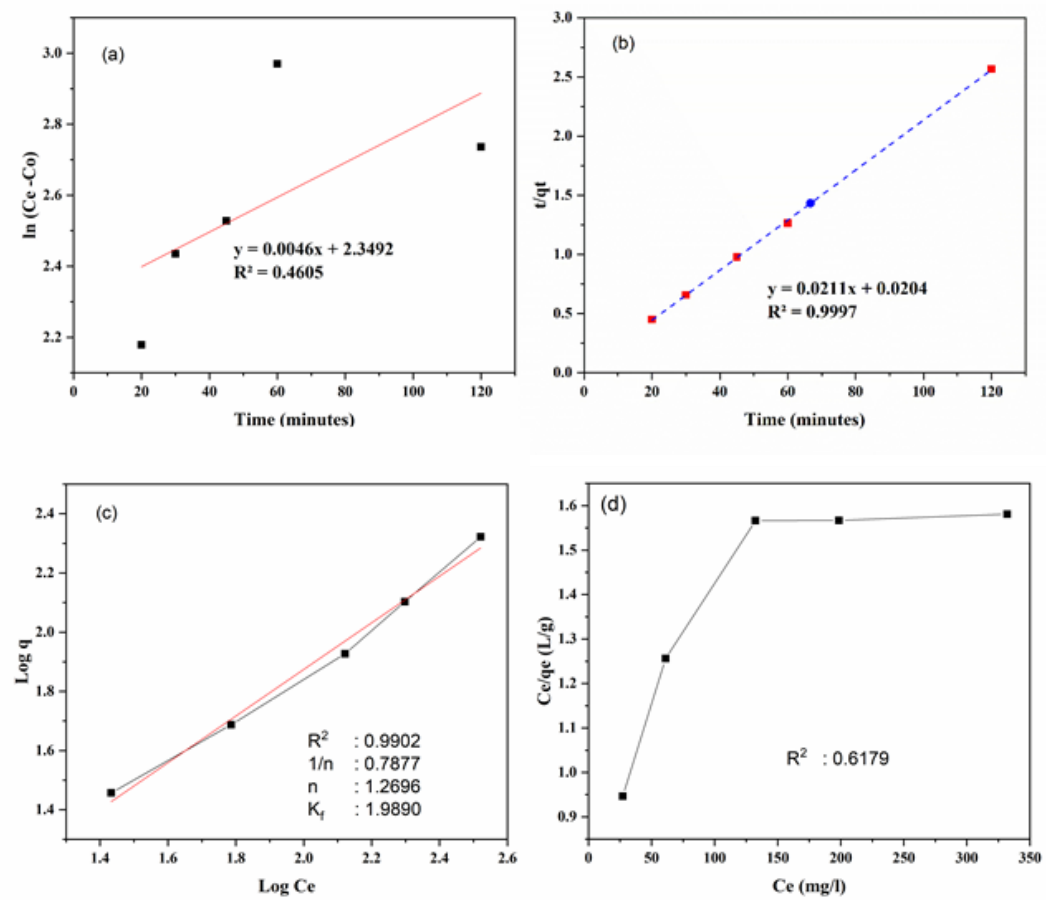

Figure 3. Adsorption kinetic and isotherm models: (a) pseudo-first-order model; (b) pseudo-second-order model; (c) Freundlich isotherm; (d) Langmuir isotherm

FTIR Characterization

The comparison of FTIR spectra of Gamalama volcanic soil before and after Pb(II) adsorption showed no significant shifts in the characteristic vibrational bands of Si–O, Al–O, and OH groups. This behavior indicates that the main mineral framework remained structurally stable during adsorption. In Figure 4, characteristic clay peaks and several major minerals present in Gamalama volcanic soil are observed. The clay minerals identified in the sample include allophane, halloysite, and kaolinite. The FTIR spectral data of GVS before adsorption exhibited three bands corresponding to hydroxyl peaks at 3687, 3618, and 3437 cm^{-1} [38], [39]. These three peaks correspond to Si–OH, Al–OH, and –OH from water. The peak at 3687 cm^{-1} was assigned to Al–OH symmetric stretching, which became slightly broader and showed a decrease in intensity after Pb adsorption. This phenomenon may be attributed to the interaction between –OH groups on the soil surface and Pb(II) ions [40], [41], [42], [43].

The Si–O–Si stretching vibration was identified by the appearance of a peak within the range of 1000–1100 cm^{-1}, while the Si–O–Al vibration appeared in the region of 520–570 cm^{-1}. These peaks did not show any shift after Pb adsorption, indicating that the aluminosilicate framework remained stable and intact [44], [45]. However, a noticeable decrease in peak intensity was observed in the FTIR data. This may correspond to a possible interaction between Pb^{2+} ions and the aluminosilicate surface. This confirms the occurrence of chemisorption on the adsorbent, likely through surface complexation (≡Al–O–Pb and ≡Si–O–Pb), and is consistent with the kinetic and isotherm data described above.

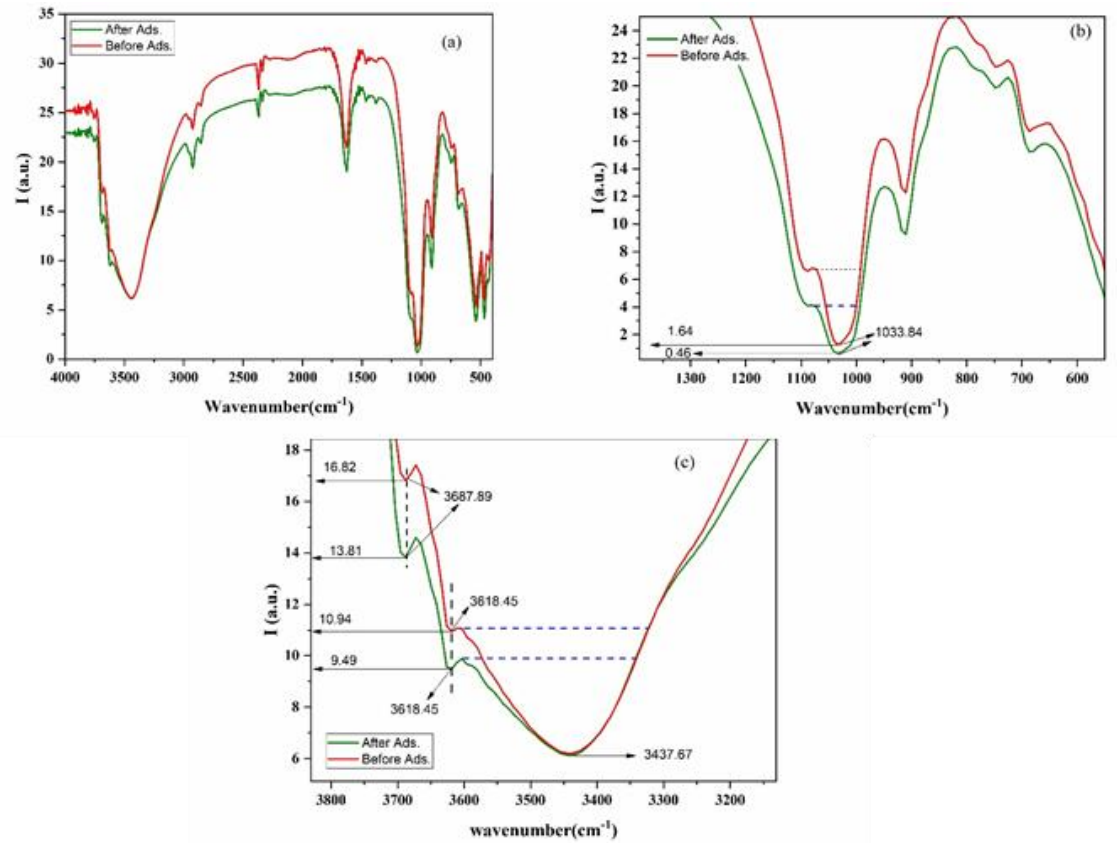

Figure 4. FTIR spectra of Gamalama volcanic soil before and after Pb adsorption

Copyright © 2026 WJC | ISSN 2621-5985 (online) | ISSN 2549-385X (print)
Volume 9, Nomor 1, 2026

XRD and SAA–BET Characterization

Figure 5. displays several characteristic diffraction peaks at 2θ = 8.827° (10 Å), 19.69° (4.5 Å), 22.09° (4.02 Å), 22.926° (3.87 Å), 26.564° (3.36 Å), 27.93° (3.20 Å), 28.55° (3.10 Å), 29.96° (2.96 Å), 35.04° (2.54 Å), and 49.76° (1.83 Å). These diffraction peaks confirmed the presence of halloysite (PDF No. 00-029-1489), allophane (PDF No. 00-038-0449), albite (PDF No. 00-001-0739), kaolinite (PDF No. 01-078-2109), and quartz (PDF No. 01-075-0443). The crystal structure of the soil minerals was preserved during the adsorption process. The main diffraction peaks appeared at similar 2θ positions in both samples, and no additional reflections corresponding to crystalline Pb phases were observed. After Pb uptake, only slight changes in peak intensity and broadening were observed, which could be ascribed to partial coverage of crystalline domains and a minor decrease in apparent crystallinity rather than the formation of new crystalline Pb compounds [43], [46]. The absence of new diffraction peaks may also indicate that Pb(II) is present in an amorphous or highly dispersed form on the GVS surface, which is not detectable by XRD analysis.

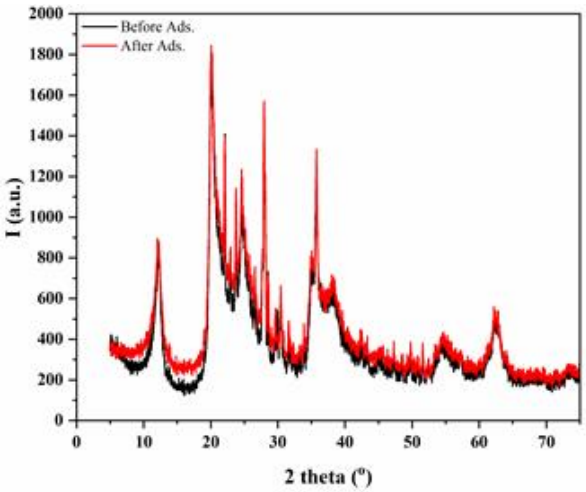

Figure 5. XRD pattern of Gamalama volcanic soil before and after Pb adsorption

These data, combined with FTIR and the pseudo-second-order/Freundlich adsorption behavior, suggest that Pb was predominantly retained through surface complexation on Al–O–H and Si–O–H groups of the aluminosilicate matrix, forming highly dispersed, poorly crystalline Pb species on the Gamalama volcanic soil surface. In addition, no shifting of 2θ values was observed between the raw and Pb-loaded samples, indicating that no new crystalline Pb phase, such as PbO, $Pb(OH)_2$, or Pb-silicate, was formed. Only a decrease in intensity and slight peak broadening occurred around approximately 26°, 35–37°, and 50–60° 2θ, indicating that Pb was adsorbed only on the surface without altering the crystalline lattice of the soil minerals. These observations are strongly supported by the FTIR results. Broadening and a decrease in the intensity of the –OH stretching band at approximately 3400 cm^{-1} were observed without any peak shift, indicating surface complexation rather than lattice substitution. This evidence is consistent with the pseudo-second-order kinetic model (R^2 = 0.9997), suggesting chemisorption as the rate-controlling mechanism. Based on the combined kinetic, isotherm, FTIR, and XRD results, the adsorption of Pb(II) onto GVS is proposed to occur through a combination of electrostatic interactions, surface complexation with

hydroxyl groups (≡Si–OH and ≡Al–OH), and possible ion exchange mechanisms.

BET analysis of Gamalama volcanic soil before and after Pb adsorption showed changes in its surface properties. The results of this analysis indicate that the adsorption process occurred primarily on the surface of the adsorbent and was not caused by changes in the GVS mineral structure. The specific surface area decreased from 490.128 to 464.707 m^2/g. This decrease indicates that Pb^{2+} ions occupied active sites on the GVS surface, causing some pores to become blocked and reducing the number of sites available for adsorption. This finding is consistent with the results of the kinetic analysis, which followed the pseudo-second-order model (R^2 = 0.9997), indicating that the adsorption process was dominated by chemisorption in the form of interactions between Pb^{2+} ions and Al–O/Si–O functional groups on the surface of GVS minerals. These results also support the adsorption isotherm analysis, which showed better agreement with the Freundlich isotherm (R^2 = 0.9902), indicating that the adsorption process occurred on a heterogeneous surface in a multilayer system. The XRD characterization results before and after adsorption did not show a 2θ shift, indicating that Pb ions were bound only to the GVS surface.

This finding is consistent with the BET data, which showed a decrease in the specific surface area after adsorption. Overall, the results of this study indicate that Pb adsorption occurs through surface interactions and pore blockage without damaging the basic aluminosilicate structure of Gamalama volcanic soil. This property is commonly found in volcanic soils rich in allophane and halloysite, such as GVS, which have high surface areas, numerous active groups, and good metal ion binding capacity [42], [44], [47]. With these characteristics, Gamalama volcanic soil has good potential as a stable natural adsorbent and can be used to help reduce heavy metal pollution in water.

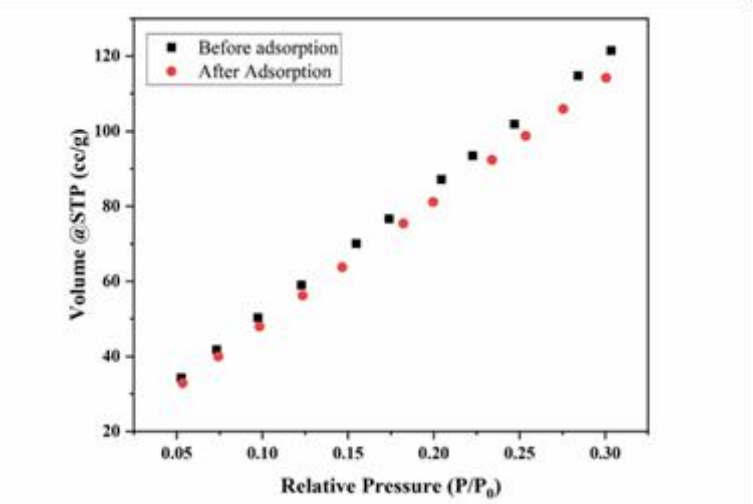

Figure 6. BET isotherm of Gamalama volcanic soil before and after Pb adsorption

Conclusion

The adsorption of Pb(II) onto GVS followed the pseudo-second-order kinetic model and the Freundlich isotherm, indicating chemisorption on heterogeneous surfaces. XRD results showed no significant changes in the main diffraction patterns after adsorption, suggesting that the bulk structure of GVS remained largely unchanged, although further characterization is needed for confirmation. The Pb(II) adsorption capacity of GVS was 140 mg/g, highlighting the potential of GVS as a low-cost adsorbent for Pb(II) removal. Future studies should explore its selectivity,

regeneration, and application in real wastewater systems.

Acknowledgement

This research was financially supported by the Higher Education Competitive Excellence Research Program (PKUPT), Faculty of Teacher Training and Education, Universitas Khairun, Ternate, under grant number 012/PEN-PKUPT/PG.12/2025.

References

[1] N. A. A. Qasem, R. H. Mohammed, and D. U. Lawal, "Removal of heavy metal ions from wastewater: a comprehensive and critical review," npj Clean Water 2021 4:1, vol. 4, no. 1, pp. 1–15, Jul. 2021, doi: 10.1038/s41545-021-00127-0.

[2] V. L. Kapepula and P. Luis, "Removal of heavy metals from wastewater using reverse osmosis," Frontiers in Chemical Engineering, vol. 6, p. 1334816, Feb. 2024, doi: 10.3389/fceng.2024.1334816

[3] A. El Mouden et al., "Removal of cadmium and lead ions from aqueous solutions by novel dolomite-quartz@Fe_3O_4 nanocomposite fabricated as nanoadsorbent," Environ. Res., vol. 225, May 2023, doi: 10.1016/j.envres.2023.115606.

[4] J. A. Alexander, M. A. Ahmad Zaini, A. Surajudeen, E. N. U. Aliyu, and A. U. Omeiza, "Insight into kinetics and thermodynamics properties of multicomponent lead(II), cadmium(II) and manganese(II) adsorption onto Dijah-Monkin bentonite clay," Particulate Science and Technology, vol. 36, no. 5, pp. 569–577, Jul. 2018, doi: 10.1080/02726351.2016.1276499

[5] A. Zehhaf, A. Benyoucef, R. Berenguer, C. Quijada, S. Taleb, and E. Morallon, "Lead ion adsorption from aqueous solutions in modified Algerian montmorillonites," J. Therm. Anal. Calorim., vol. 110, no. 3, pp. 1069–1077, Dec. 2012, doi: 10.1007/s10973-011-2021-8.

[6] M. C. Benalia, L. Youcef, M. G. Bouaziz, S. Achour, and H. Menasra, "Removal of Heavy Metals from Industrial Wastewater by Chemical Precipitation: Mechanisms and Sludge Characterization," Arab. J. Sci. Eng., vol. 47, no. 5, pp. 5587–5599, May 2022, doi: 10.1007/s13369-021-05525-7.

[7] A. Dąbrowski, Z. Hubicki, P. Podkościelny, and E. Robens, "Selective removal of the heavy metal ions from waters and industrial wastewaters by ion-exchange method," Chemosphere, vol. 56, no. 2, pp. 91–106, 2004, doi: 10.1016/j.chemosphere.2004.03.006.

[8] A. Oehmen, D. Vergel, J. Fradinho, M. A. M. Reis, J. G. Crespo, and S. Velizarov, "Mercury removal from water streams through the ion exchange membrane bioreactor concept," J. Hazard. Mater., vol. 264, pp. 65–70, Jan. 2014, doi: 10.1016/j.jhazmat.2013.10.067.

[10] M. Makaremi, R. T. De Silva, and P. Pasbakhsh, "Electrospun nanofibrous membranes of polyacrylonitrile/halloysite with superior water filtration ability," Journal of Physical Chemistry C, vol. 119, no. 14, pp. 7949–7958, 2015, doi: 10.1021/acs.jpcc.5b00662.

[11] H. A. Qdais and H. Moussa, "Removal of heavy metals from wastewater by membrane processes: a comparative study," Desalination, vol. 164, no. 2,

pp. 105–110, Apr. 2004, doi: 10.1016/S0011-9164(04)00169-9.

[12] M. Y. Chong and Y. J. Tam, "Bioremediation of dyes using coconut parts via adsorption: a review," SN Appl. Sci., vol. 2, no. 2, pp. 1–16, Feb. 2020, doi: 10.1007/s42452-020-1978-y.

[13] Z. Li et al., "Adsorption of methylene blue on silica nanoparticles: Modelling analysis of the adsorption mechanism via a double layer model," J. Mol. Liq., vol. 319, 2020, doi: 10.1016/j.molliq.2020.114348.

[14] G. Vilardi, L. Di Palma, and N. Verdone, "Heavy metals adsorption by banana peels micro-powder: Equilibrium modeling by non-linear models," Chin. J. Chem. Eng., vol. 26, no. 3, pp. 455–464, 2018, doi: 10.1016/j.cjche.2017.06.026.

[15] C. Y. Tahya, M. Cornelia, T. M. Siregar, and M. I. Taipabu, "Adsorption of Copper Ion from Acidic Wastewater by Local Natural Zeolite," Walisongo Journal of Chemistry, vol. 5, no. 2, pp. 136–144, Dec. 2022, doi: 10.21580/wjc.v5i2.11714.

[16] K. Kustomo, N. L. Z. Faza, and A. Haarstrick, "Adsorption of Cd (II) into Activated Charcoal from Matoa Fruit Peel," Walisongo Journal of Chemistry, vol. 5, no. 1, pp. 83–93, Jul. 2022, doi: 10.21580/wjc.v5i1.11755.

[17] I. Cipta, F. Febiyanto, A. Syoufian, and I. Kartini, "Identification and Characterization of Nanoclays in Gamalama Volcanic Soil of Northern Maluku," Clays Clay Miner., vol. 70, no. 3, pp. 438–449, Jun. 2022, doi: 10.1007/s42860-022-00190-9.

[18] N. A. Limatahu, I. Cipta, St. H. Nur Abu, I. Kartini, and Y. Arryanto, "Adsorption and photodegradation of methylene blue by allophane and nanocomposite bismuth oxyiodide-allophane," Asian Journal of Chemistry, vol. 30, no. 1, 2018, doi: 10.14233/ajchem.2018.20990.

[19] I. Cipta, N. A. Limatahu, S. H. Nur Abu, I. Kartini, and Y. Arryanto, "Characterization of allophane from gamalama volcanic soil, North Maluku, Indonesia," Asian Journal of Chemistry, vol. 29, no. 8, pp. 1702–1704, 2017, doi: 10.14233/ajchem.2017.20620.

[20] I. Cipta et al., "Adsorption Kinetics Of Methyl Orange On Silica Derived From Gamalama Volcanic Soil," Walisongo Journal of Chemistry, vol. 8, no. 1, pp. 127–137, Jul. 2025, doi: 10.21580/WJC.V8I1.26066.

[21] M. Vhahangwele, & G. W. Mugera, "The potential of ball-milled South African bentonite clay for attenuation of heavy metals from acidic wastewaters: Simultaneous sorption of Co^{2+}, Cu^{2+}, Ni^{2+}, Pb^{2+}, and Zn^{2+} ions," Journal of Environmental Chemical Engineering, vol. 3, no. 4, pp. 2416–2425, Dec. 2015, doi:10.1016/J.JECE.2015.08.016

[23] S. Lagergren, (1898), "About the Theory of So-Called Adsorption of Soluble Substances," Kungliga Svenska Vetenskapsakademiens. Handlingar (Bihang till), vol.24, pp. 1-39.

[24] Y. S. Ho and G. McKay, "The sorption of lead(II) ions on peat," Water Res., vol. 33, no. 2, pp. 578–584, Feb. 1999, doi: 10.1016/S0043-1354(98)00207-3.

[25] I. Langmuir, "The Adsorption Of Gases On Plane Surfaces Of Glass, Mica And Platinum," J. Am. Chem. Soc., vol. 40, no. 9, pp. 1361–1403, Sep. 2002, doi: 10.1021/JA02242A004.

[26] H. Freundlich, "Over the adsorption in solution," Zeitschrift für Physikalische Chemie, vol. 57(1), pp. 385–470, 1906.

[27] V. P. Dinh et al., "HTDMA-modified bentonite clay for effective removal of Pb(II) from aqueous solution," Chemosphere, vol. 286, Jan. 2022, doi: 10.1016/j.chemosphere.2021.131766.

[28] Y. Chuang et al., "Sorption studies of Pb(II) onto montmorillonite clay," IOP Conf. Ser. Earth Environ. Sci., vol. 1087, no. 1, p. 012007, Oct. 2022, doi: 10.1088/1755-1315/1087/1/012007.

[29] Y. Laidani, G. Henini, S. Hanini, and A. Fekaouni, "Study of the Kinetics and Thermodynamics of Adsorption of Hexavalent Chromium on the Luffa Cylindrica Cords," Iran. J. Chem. Chem. Eng., vol. 39, no. 4, 2020, doi: 1021-9986/2020/4/137-151.

[30] Z. Han, Y. Zhang, S. Zheng, J. Chen, Y. Zhang, and X. Yue, "Pb^{2+} Removal from Aqueous Solutions Using Montmorillonite and Magnetite-Modified Nanostructures," Water Air Soil Pollut., vol. 236, no. 7, Jul. 2025, doi: 10.1007/s11270-025-08070-3.

[31] H. Hadjar, A. C. Mammar, T. Harouche, T. Yahia, and N. Kichou, "Design of Mg–Al layered double hydroxides for lead capture from polluted water: kinetics, isoelectric point, and pH effect," International Journal of Environmental Science and Technology, vol. 22, no. 1, pp. 171–188, Jan. 2025, doi: 10.1007/s13762-024-05824-0.

[32] G. Li, J. Zhang, and J. Liu, "Adsorption characteristics of Pb (II) onto red clay, bentonite and bone char," in IOP Conference Series: Earth and Environmental Science, Institute of Physics Publishing, Jul. 2020. doi: 10.1088/1755-1315/526/1/012018.

[33] H. Wang, J. Wang, Z. Wang, Q. Ye, and J. Zhang, "Characterization and adsorption properties of rectorite/sludge-derived biochar composites for Pb(II) removal," Adsorption Science and Technology, vol. 42, Jan. 2024, doi: 10.1177/02636174241287698.

[34] M. Yuan, T. Xie, G. Yan, Q. Chen, and L. Wang, "Effective removal of Pb^{2+} from aqueous solutions by magnetically modified zeolite," Powder Technol., vol. 332, pp. 234–241, Jun. 2018, doi: 10.1016/J.POWTEC.2018.03.043.

[35] M. Anbia, K. Kargosha, and S. Khoshbooei, "Heavy metal ions removal from aqueous media by modified magnetic mesoporous silica MCM-48," Chemical Engineering Research and Design, vol. 93, pp. 779–788, Jan. 2015, doi: 10.1016/J.CHERD.2014.07.018.

[36] V. Hernández-Montoya, M. A. Pérez-Cruz, D. I. Mendoza-Castillo, M. R. Moreno-Virgen, and A. Bonilla-Petriciolet, "Competitive adsorption of dyes and heavy metals on zeolitic structures," J. Environ. Manage., vol. 116, pp. 213–221, Feb. 2013, doi: 10.1016/J.JENVMAN.2012.12.010.

[37] T. W. Cheng, M. L. Lee, M. S. Ko, T. H. Ueng, and S. F. Yang, "The heavy metal adsorption characteristics on metakaolin-based geopolymer," Appl. Clay Sci., vol. 56, pp. 90–96, Feb. 2012, doi: 10.1016/J.CLAY.2011.11.027.

[38] D. P. Kgabi and A. A. Ambushe, "Removal of Pb(II) ions from aqueous solutions using natural and HDTMA-modified bentonite and kaolin clays," Heliyon, vol. 10, no. 18, Sep. 2024, doi: 10.1016/j.heliyon.2024.e38136.

[39] A. G. Alghamdi and Z. Alasmary, "Fate and Transport of Lead and Copper in Calcareous Soil," Sustainability

(Switzerland), vol. 15, no. 1, Jan. 2023, doi: 10.3390/su15010775.

[40] M. Fouodjouo, H. Fotouo-Nkaffo, S. Laminsi, F. A. Cassini, L. O. de Brito-Benetoli, and N. A. Debacher, "Adsorption of copper (II) onto cameroonian clay modified by non-thermal plasma: Characterization, chemical equilibrium and thermodynamic studies," Appl. Clay Sci., vol. 142, pp. 136–144, Jun. 2017, doi: 10.1016/j.clay.2016.09.028.

[41] R. Bassam et al., "Studies on the Removal of Cadmium Toxic Metal Ions by Natural Clays from Aqueous Solution by Adsorption Process," J. Chem., vol. 2021, 2021, doi: 10.1155/2021/7873488.

[42] P. Maziarz and J. Matusik, "The effect of acid activation and calcination of halloysite on the efficiency and selectivity of Pb(II), Cd(II), Zn(II) and As(V) uptake," Clay Miner., vol. 51, no. 3, pp. 385–394, Jun. 2016, doi: 10.1180/claymin.2016.051.3.06.

[43] I. Abdelfattah, W. Abdelwahab, and A. M. El-Shamy, "Montmorillonitic clay as a Cost Effective, Eco-Friendly and Sustainable Adsorbent for Physicochemical Treatment of Contaminated Water," Egypt. J. Chem., vol. 65, no. 2, pp. 687–694, Feb. 2022, doi: 10.21608/EJCHEM.2021.92320.4378.

[44] S. Kadi, S. Lellou, K. Marouf-Khelifa, J. Schott, I. Gener-Batonneau, and A. Khelifa, "Preparation, characterisation and application of thermally treated Algerian halloysite," Microporous and Mesoporous Materials, vol. 158, pp. 47–54, Aug. 2012, doi: 10.1016/j.micromeso.2012.03.014.

[45] Z. C. Kadirova, M. Hojamberdiev, L. Bo, R. Hojiyev, and K. Okada, "Simultaneous removal of NH4+, $H_2PO_4^-$ and Ni^{2+} from aqueous solution by thermally activated combinations of steel converter slag and spent alumina catalyst," Journal of Water Process Engineering, vol. 8, pp. 151–159, Dec. 2015, doi: 10.1016/j.jwpe.2015.10.004.

[46] C. P. Johnston and M. Chrysochoou, "Mechanisms of chromate adsorption on hematite," Geochim. Cosmochim. Acta, vol. 138, pp. 146–157, Aug. 2014, doi: 10.1016/j.gca.2014.04.030.

[47] P. M. Słomkiewicz, B. Szczepanik, and M. Garnuszek, "Determination of adsorption isotherms of aniline and 4-chloroaniline on halloysite adsorbent by inverse liquid chromatography," Appl. Clay Sci., vol. 114, pp. 221–228, Sep. 2015, doi: 10.1016/j.clay.2015.06.007.